

Accepted Manuscript

Oxygen reduction reaction (orr) on bimetallic AuPt and AuPd (100)–electrodes: effects of the heteroatomic junction on the reaction paths

E. Schulte, G. Belletti, M. Arce, P. Quaino

PII: S0169-4332(18)30283-6

DOI: <https://doi.org/10.1016/j.apsusc.2018.01.265>

Reference: APSUSC 38404

To appear in: *Applied Surface Science*

Received Date: 30 November 2017

Revised Date: 17 January 2018

Accepted Date: 29 January 2018

Please cite this article as: E. Schulte, G. Belletti, M. Arce, P. Quaino, Oxygen reduction reaction (orr) on bimetallic AuPt and AuPd (100)–electrodes: effects of the heteroatomic junction on the reaction paths, *Applied Surface Science* (2018), doi: <https://doi.org/10.1016/j.apsusc.2018.01.265>

This is a PDF file of an unedited manuscript that has been accepted for publication. As a service to our customers we are providing this early version of the manuscript. The manuscript will undergo copyediting, typesetting, and review of the resulting proof before it is published in its final form. Please note that during the production process errors may be discovered which could affect the content, and all legal disclaimers that apply to the journal pertain.



Oxygen reduction reaction (orr) on bimetallic AuPt and AuPd (100)–electrodes: effects of the heteroatomic junction on the reaction paths

E. Schulte¹, G. Belletti¹, M. Arce², P. Quaino^{1,*}

¹Instituto de Química Aplicada del Litoral, IQAL (UNL-CONICET), PRELINE (FIQ-UNL), Santa Fe, Argentina

²CNEA-CONICET, Centro Atómico Bariloche, Av. Bustillo 9500, S. C. de Bariloche, Rio Negro, 8400, Argentina

*Corresponding author

Abstract

The seek for materials to enhance the oxygen reduction reaction (orr) rate is a highly relevant topic due to its implication in fuel cell devices. Herein, the orr on bimetallic electrocatalysts based on Au-M (M= Pt, Pd) has been studied computationally, by performing density functional theory calculations. Bimetallic (100) electrode surfaces with two different Au:M ratios were proposed, and two possible pathways, associative and dissociative, were considered for the orr. Changes in the electronic properties of these materials with respect to the pure metals were acknowledged to gain understanding in the overall reactivity trend. The effect of the bimetallic junction on the stability of the intermediates O₂ and OOH was also evaluated by means of geometrical and energetic parameters; being the intermediates preferably adsorbed on Pt/Pd atoms, but presenting in some cases higher adsorption energies compared with bare metals. Finally, the kinetics of the O–O bond breaking in O₂^{*} and OOH^{*} adsorbed intermediates in the bimetallic materials and the influence of the Au-M junction were studied by means of the nudge elastic-band method. A barrierless process for the scission of O₂^{*} was found in Au-M for the higher M ratios. Surprisingly, for Au-M with lower M ratios, the barriers were much lower than for pure Au surfaces, suggesting a highly reactive surface towards the orr. The O–O scission of the OOH^{*} was found to be a barrierless process in Au-Pt systems and nearly barrierless in all Au-Pd systems, implying that the reduction of O₂ in these systems proceeds via the full reduction of O₂ to H₂O, avoiding H₂O₂ formation.

Keywords: oxygen reduction reaction, DFT, bimetallic electrocatalysts, cathode, fuel cell.

1 Introduction

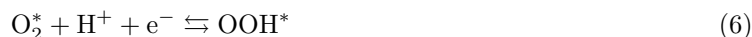
The oxygen reduction reaction (orr) is one of the most important reactions in electrochemistry and fuel cell technologies [1, 2, 3, 4]. It takes place in the cathode of most fuel cell devices currently designed, and shows a highly complex behavior, which depends on the electrode material and electrolyte. The full 4e⁻ reduction of oxygen to water can occur via two parallel pathways, known as Direct (or Dissociative) and Serial (or Associative) mechanism. A secondary reaction can occur, which is the 2e⁻ reduction of oxygen to hydrogen peroxide, known as the "peroxide route" [5]. Although innumerable experimental studies have been carried out on noble [6, 7, 8, 9] and non-noble [10, 11, 12] metals, alloys [13, 14, 15, 16], etc., unfortunately, they do not give a consistent picture of the reaction mechanism and their results are still under debate [5, 17]. In principle, considering the simultaneous occurrence of both routes, the mechanism of the orr in acid media could proceed through different adsorbed intermediates on active sites on the metal electrode which determine the final products, H₂O and/or H₂O₂.

Several mechanisms can be proposed for the reaction: dissociative, associative, peroxide and aquoxyl mechanisms [18]. Two of them - the dissociation of oxygen or peroxy - are described below (being * the active metal adsorption site), where the scission of the O–O (O–OH) bond (i.e. steps 2 and 7) will be the focus of our studies:

Dissociative mechanism (O₂)



Associative mechanism (OOH)



Although in principle, both mechanisms lead to the same product for the full 4e^- reduction of $\text{O}_{2(\text{dis})}$ (i.e. water), the associative mechanism can also lead to the suboptimal 2e^- reduction of $\text{O}_{2(\text{dis})}$ producing H_2O_2 ($\text{OOH}^* + \text{H}^+ + \text{e}^- \rightleftharpoons \text{H}_2\text{O}_2$ (10)). This unwanted by-product has two main issues, on the one hand is less energy-efficient for power generation in PEMFC; on the other hand, hydrogen peroxide can lead to faster degradation of fuel cell components. Thus, if the associative mechanism is hindered by the electrocatalyst, the secondary reaction is suppressed.

During the years, much information has been collected concerning the search and improvement of electrode materials [19]. Indeed, one of the most urgent problems of the fuel cell technology is to find a better catalyst for the oxygen reduction. Currently, Pt-based materials are the best known catalysts for the orr, but also highly expensive and scarce [20, 21]. Over the years, several materials and combinations have been proposed aiming to enhance the electrocatalyst performance, while replacing Pt or at least decreasing its loading [22, 23, 24, 25]. However, due to the complexity of the reaction itself, and beyond every attempt to improve the efficiency of the device, there is still a lack of understanding in the fundamental processes of the reaction; being this scenario the major source of inefficiency in fuel cells. One of the crucial points is to delve into the knowledge of mechanistic aspects that determine the electrocatalytic activity of the electrode materials, since it would help in their rational design. The possible reaction routes and the behavior of the adsorbed species, such as intermediates and/or inhibitors, must be clearly understood. Thus, a smart selection of materials for which the reaction proceeds mainly through the most appropriate route can be consciously achieved [26, 4, 27]. Regarding this matter, many studies have been oriented to modify the electronic properties of the adsorption sites on pure electrodes such as the adsorption of metal adatoms [28, 29], surface facetting [30, 31], core-shell nanoparticles [32, 33], etc. However, not always a direct correlation exists between the tuning of the material and a significant change in its electrocatalytic activity for a specific reaction.

Many experimental and theoretical works have studied binary superlattice materials, as some of these hybrid systems exhibit better properties than the isolated constituents, due to the existence of synergistic effects between them [34, 35, 36]. From a theoretical perspective, the design of hybrid materials with heteroatomic junctions, with the maximum ratio between mixed and pure sites, provides a powerful alternative for the study of reactions involving more than one adsorbed intermediate, illustrative examples of these kind of systems can be found in literature [37, 38]. The oxygen reduction reaction seems to be a case where the presence of active sites with different functions would benefit the electrocatalytic activity. In this sense, some attempts have been made to develop a bifunctional model of a more efficient mechanism for the reaction based on both, macroscopic thermodynamic properties [39] and ab-initio calculations [40], where a metal (M1) favors the O_2 bond breaking and the bond formation of the intermediate (M1-O), while the other metal (M2) favors the intermediate electrooxidation to water. Obviously, this is a simplified view of the process, which serves only as a guideline for the design of possible materials. In this context, some bimetallic electrodes have shown superior performances for the orr than each pure material [41, 42, 43, 44, 45, 46].

Herein, computational studies based on density functional theory (DFT) have been performed to clarify energetic and electronic effects governing the reactivity of bimetallic electrode material for the oxygen reduction reaction (orr). The studies are particularly oriented to the interfacial line generated by the combination of two metals in contact (nPd/mAu, nPt/mAu). Additionally, we have investigated the effect of the bimetallic junction on the activation barriers for specific kinetic processes that govern the orr, specifically the scission of the O-O bond in two type of molecular precursors $\text{O}_{2\text{ad}}$ and OOH_{ad} . This paper is organized as follows. Some pertinent details on model calculations are reported in the next section. Then, we present the results of DFT calculations to evaluate the effect of the bimetallic junction on the selectivity of the adsorption process. Different adsorbed intermediates, adsorption environments,

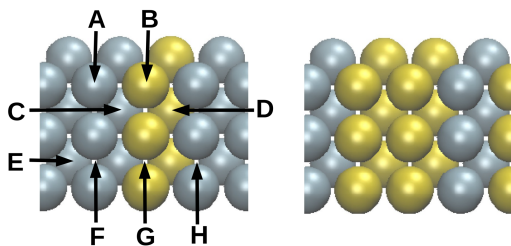


Figure 1: Top view of the bimetallic electrodes (geometrical pattern). Left side: 2M/1Au. Right side: 1M/2Au. M=Pt, Pd. The gray spheres correspond to Pd or Pt atoms whereas the yellow ones correspond to atoms of Au. The adsorption sites were identified as follows: A) M top site. B) Au top site. C) 4-fold mixed hollow site, M atom underneath the first surface layer. D) 4-fold mixed hollow site, Au atom underneath the first surface layer. E) 4-fold M hollow site. F) M bridge site. G) Au bridge site. H) M mixed bridge site.

and electronic effects are estimated and analyzed. Kinetic processes of our interest are investigated, and their energy barriers are addressed as well. Concluding remarks are reported in the last section.

2 DFT calculations and modeling

Periodic DFT calculations were performed using VASP code [47, 48, 49]. The core electrons were kept frozen and replaced by pseudopotentials generated by the plane augmented wave method (PAW) [50, 51, 52, 53]. The outermost shell were treated by means of a plane-wave basis set with a cutoff of 450 eV. The electron–electron exchange and correlation interactions were treated with the generalized gradient approximation (GGA) in the version of Perdew and Wang [54]. The application of this functional on bulk Pt, Pd and Au results in theoretical lattice parameters of $a_0^{\text{Pt}} = 3.96 \text{ \AA}$, $a_0^{\text{Pd}} = 3.98 \text{ \AA}$, and $a_0^{\text{Au}} = 4.18 \text{ \AA}$. Within the typical margins of errors, both constants agree with the experimental data $a_0^{\text{Pt}} = 3.92 \text{ \AA}$, $a_0^{\text{Pd}} = 3.89 \text{ \AA}$, and $a_0^{\text{Au}} = 4.08 \text{ \AA}$ reported in the literature [55]. For the mixed surfaces, an average lattice constant between both metals was taken to build the surfaces [56]. For all the systems, the two bottom layers were fixed at the next-neighbor distance corresponding to bulk and all the other layers were allowed to fully relax. The convergence criterion was achieved when the total forces were less than 0.02 eV/\AA . In all the calculations a vacuum corresponding to 20 \AA was used. The parametrization of the k-points sampling of the Brillouin zone based on the Monkhorst-Pack grid [57] was considered. The parameters were increased systematically until the change in the absolute energy was less than 10 meV . A grid of $(7 \times 7 \times 1)$ k-points was used for a (3×3) unit cell. In all the calculations spin polarization was considered.

As explained previously, we are focused on the scission of the O–O (O–OH) bond, which avoids the hydrogen peroxide formation. Thus, the adsorption of O_2 and OOH, considered precursors for their dissociation process, was performed on two types of systems: pure metal surfaces – Pt(100), Pd(100) and Au(100) – and bimetallic superlattices – nM/mAu, M=Pt, Pd. The pure metal surfaces were modeled by a (3×3) supercell with 4 metal layers. To model the bimetallic nM/mAu electrodes, (3×3) supercells with 4 layers were used. To consider the effect of the amount of atoms in the new material on the reaction intermediates two different nM/mAu ratios were studied. Thus, two structures for each combination were checked: 1M/2Au, 2M/1Au, M=Pt, Pd. Fig. 1 shows a representative picture of the geometrical pattern for each combination of Pd or Pt with Au atoms considered in the present study. The adsorption was investigated in all the sites shown in Fig. 1 for each system, and the most favorable ones are reported in this contribution. The classification of the new adsorption sites originated by the bimetallic combination is also reported (Fig. 1).

Kinetic processes of our interest were evaluated using the nudged elastic-band (NEB) method [58, 59] to find the minimum energy paths and the corresponding activation barriers using seven images of the system along the transition path. Within this method the initial and final states are known and a chain of beads is connected by harmonic springs ($k = 0.1 \text{ eV \AA}^{-2}$) between reactant and product states. Each transition state have been verified to have a single imaginary frequency. The general parameters used for the NEB calculations are the same as those for the previous DFT calculations described above. For relaxations, the convergence criterion was achieved when the total forces were less than 0.02 eV/\AA .

3 Results

3.1 Energetics. Influence of the bimetallic junction on the adsorption.

To begin with, we have investigated the changes in the electronic properties of the bimetallic materials to understand the surface reactivity. A comparison of the d bands for each systems – n Pd/ m Au and n Pt/ m Au – with the bare metal (100) surfaces – Pd, Pt, Au – is shown in Fig. 2. The DOS of the d bands changes gradually with the amount of Pd or Pt incorporated to the Au surface. As expected due to the similarities of both metals for belonging to the same group in periodic table (Pd, Pt) the behavior of the DOS is highly alike, although more pronounced changes are detected for the Pd profiles. In general, for both bimetallic materials, the d band appears to be shifted to more positive energies (Fig. 2: green (1M/2Au) and blue (2M/1Au) lines) compared to the pure Au surface (Fig. 2: red dashed line). Geometrical factors plus the chemical interplay due to the direct contact at the bimetallic junction causes a change in the electronic properties. Therefore, it is expected that the d band profiles for the bimetallic electrodes tend to the d band of palladium or platinum when the proportion of each metal rises, due to the lesser gold influence. The upshift of the d bands to more positive energies is generally associated with a higher reactivity, indeed the presence of Pd or Pt shift the Au d band to the Fermi level, leading to an improvement in the chemisorption properties.

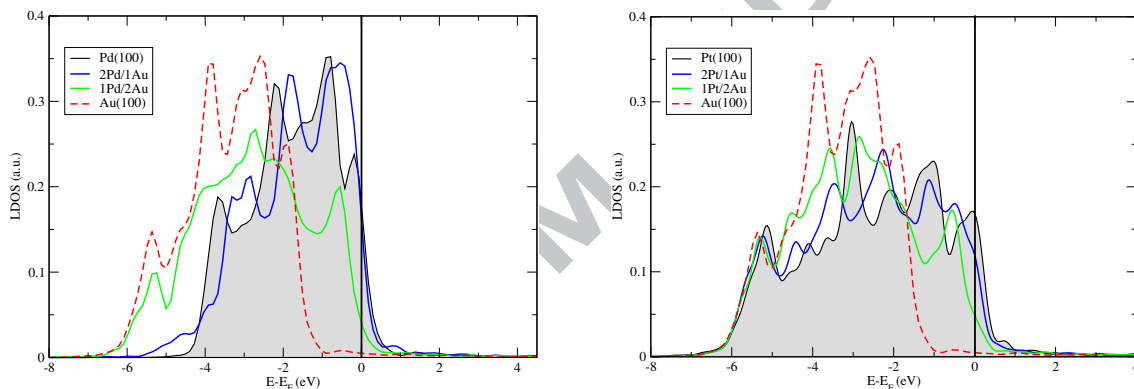


Figure 2: Projected Density of States (LDOS) on the d band of the first metal layer. Left side: Pd (100) (black line and gray area), 2Pd/1Au (blue line), 1Pd/2Au (green line) and Au (100) (red dashed line). Right side: Pt (100) (black line and gray area), 2Pt/1Au (blue line), 1Pt/2Au (green line) and Au (100) (red dashed line). The vertical line indicates the Fermi level taken as a reference.

Although the analysis of the electronic structure let us conclude that the presence of Pt or Pd increases the reactivity respect to pure Au, it is not enough to define the performance of a material as an electrocatalyst for a specific reaction. In our case, the attention is focused on the bimetallic junction, which allows to tune the shift of the d band to the Fermi level and improve the material properties. Thus, the smart selection and combination of two metals, which exhibit different behavior for the orr such as Pt and Au [60, 39] or Pd and Au [61, 62], allow to consider a modification in the reaction mechanism, leading to a change in the reactivity/selectivity due to the presence of the bimetallic interface.

In this context, we have systematically investigated the adsorption of two possible precursors for the O–O (O–OH) bond breaking, i.e. O₂ (oxygen) and OOH (peroxyl), on the mixed materials to evaluate the influence of the bimetallic junction on the adsorption properties. For comparison, the pure surfaces – Pt(100), Pd(100) and Au(100) – have been considered as references. The adsorption energy (E_{ad}) has been calculated using the following expression:

$$E_{ad}^{prec} = E_{prec/mM/nAu} - E_{mM/nAu} - E_{prec} \quad (10)$$

The first term corresponds to the energy of the relaxed system – prec/ m M/ n Au – with the precursor (prec = OOH or O₂) at the adsorption equilibrium position on the surface, the second term corresponds to the energy of the relaxed m M/ n Au surface without the precursor; the third term is the energy of the precursor in gas phase. Calculated energy values for the most favorable sites for each system are shown in Fig. 3.

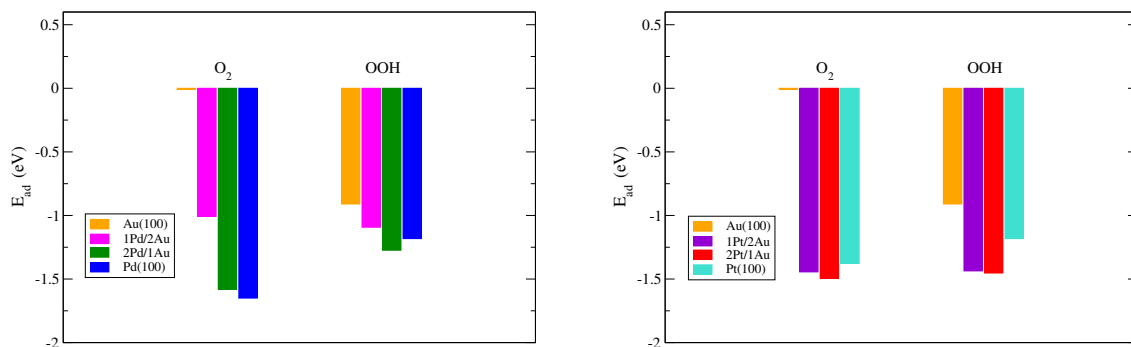


Figure 3: Adsorption energies in eV for each species OOH and O₂ on all the investigated materials. Left side: mPd/nAu, Pd, Au. Right side: mPt/nAu, Pt, Au. The energy values correspond to the most stable adsorption site.

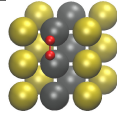
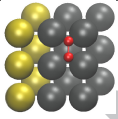
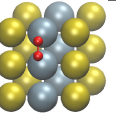
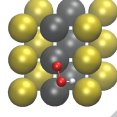
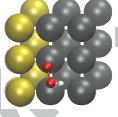
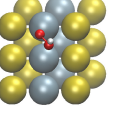
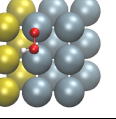
Prec	Structures	1Pd/2Au	2Pd/1Au	1Pt/2Au	2Pt/1Au
		O ₂			
OOH					

Table 1: Most stable adsorption sites for O₂ and OOH on the bimetallic structures: mPd/nAu and mPt/nAu.

Our results indicate that the adsorption process of both precursors is more favored on 1Pt/2Au and 2Pt/1Au in comparison with the pure surfaces (Pt and Au), see Fig. 3. On both systems, the behavior of OOH and O₂ follows the same trend: $E_{ad}^{prec}/2Pt/1Au < E_{ad}^{prec}/1Pt/2Au < E_{ad}^{prec}/Pt < E_{ad}^{prec}/Au$. The adsorption energies of OOH and O₂ on the pure surfaces are in agreement with the ones reported in the literature [40, 63, 64, 65]. After adsorption, the precursors were found located on "H" sites (Fig. 1) on both materials, 1Pt/2Au and 2Pt/1Au (see Table 1, right side). A higher affinity for Pt than Au is detected, which is in line with the behavior of the species on the pure metals, see E_{ad} in Fig. 3, right plot. For the sake of completeness, Fig. 4 shows the charge density difference for the O₂-mPt/nAu. Clearly, main charge accumulation in the O₂-mPt bond region and the unperturbed gold atoms confirms our previous observation. A similar behavior (not shown in the present contribution) has been found for the other systems - OOH-mPt/nAu. Finally, it should be notice that the presence of gold in these mixed materials improves significantly the adsorption, not only with respect to pure gold but with respect to pure Pt at the studied proportions.

For the case of mPd/nAu surfaces, a slightly different behavior has been found. The adsorption phenomenon was improved with respect to gold for both species (OOH and O₂) according to (less

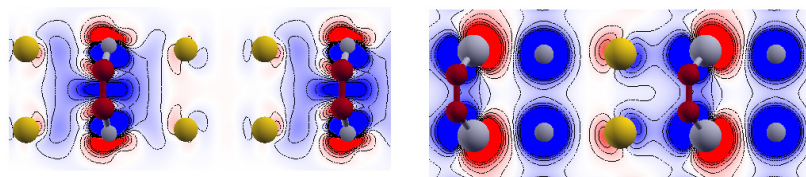


Figure 4: Cross section of the charge density difference of the O₂-mPt/nAu bond. Cut in the plane perpendicular O₂-mPt/nAu bond. Left side: O₂-1Pt/2Au. Right side: O₂-2Pt/1Au. The accumulation of charge is in red, and the depletion in blue for charge density difference.

negative energy value): $2\text{Pd}/1\text{Au} < 1\text{Pd}/2\text{Au} < \text{Au}$. Hence, the higher the amount of Pd atoms in the gold substrate, the better the adsorption properties in a similar way as in mPt/nAu systems. However, a comparison with a pure palladium surface exhibits a different scenario. The OOH adsorption energies decreases (less negative value) in the following order: $2\text{Pd}/1\text{Au} < \text{Pd} < 1\text{Pd}/2\text{Au} < \text{Au}$. In the cases of the mixed configurations, the OOH adsorption is favored on "H" sites (Table 1), and on bridge sites for bare Au and Pd in agreement with the reported data [65, 40]. For the oxygen adsorption, energetics indicates that the most stable structure for pure Pd(100) is on a hollow position in accord with [63]. The adsorption on the bimetallic configurations is strongly enhanced compared with gold surfaces. Therefore, as the presence of Pd atoms increases, the chemisorption properties are improved in the order: 1) Au, 2) $1\text{Pd}/2\text{Au}$, 3) $2\text{Pd}/1\text{Au}$. The molecule is located on bridge sites on Au and $1\text{Pd}/2\text{Au}$ surfaces ("H" site, Table 1), whereas it was found adsorbed on hollow sites at Pd and $2\text{Pd}/1\text{Au}$ structures ("E" site, Table 1).

3.2 Kinetics. Influence of the bimetallic junction on the scission of O–O and O–OH bonds.

There is an extensive literature on theoretical and computational work about different bimetallic surfaces [41, 42, 43, 44, 66, 67, 68, 69] and the oxygen reduction reaction on such electrocatalysts [44, 69, 70, 71, 72]. For instance, the work of Zhang *et al.* can be cited, where the authors showed an enhancement of the ORR kinetics on a mixed monolayer of Pt and another transition metal (Ir, Ru, Rh, Pd, Au, Re, Os) deposited on a (111) Pd substrate [69].

Specifically in this occasion, we were motivated to find a change in the reactivity/selectivity of a bimetallic material due to the metal composition and geometrical arrangement (heteroatomic junction). In this regard, we propose an intercalated configuration that increases the intermetallic interaction, maximizing the contact line between two metals. Also, working with two different compositions and combinations ($1\text{Pt}/2\text{Au}$, $2\text{Pt}/1\text{Au}$ and $1\text{Pd}/2\text{Au}$, $2\text{Pd}/1\text{Au}$) allows to appreciate the contribution of each metal on the kinetics, and if possible to establish a composition–reactivity trend.

A comparative study of the material electrocatalytic capacity for a given reaction can be accomplished by analyzing the dissociation energy [73]. In line with our interest for designing an optimal material, the formation of hydrogen peroxide must be prevented. Hence, due to the complex nature of the oxygen reaction, we shall consider two specific steps as a starting point to avoid the H_2O_2 generation: the bond breaking of $\text{O}_{2(\text{ad})}$ – into $2\text{O}_{(\text{ad})}$ – and, the bond breaking of $\text{OOH}_{(\text{ad})}$ – into $\text{O}_{(\text{ad})}$ and $\text{OH}_{(\text{ad})}$. Thus, as a first approach, the scission energy provides valuable information regarding the material performance. This simple idea helps to improve the *in silico* design of catalysts, especially for the screening of a large number of materials. Obviously, after a pre-selection is done, further theoretical, computational and experimental studies should be performed with the selected materials and geometrical structures to have a deeper understanding.

Oxygen reaction mechanisms have been deeply studied for various electrocatalysts and are well documented [74]. As described above, due to the complexity of the reaction, several mechanisms have been proposed and many approaches can be found in the literature [75]; but to the best of our knowledge, there are still some aspects of the reaction which remain unclear. Therefore, as a starting point, we have considered the two steps mentioned previously (2 and 7): the dissociation (or bond breaking) of $\text{O}_{2(\text{ad})}$ and $\text{OOH}_{(\text{ad})}$ on pure¹ and mixed surfaces: Pd(100), Pt(100), Au(100), $1\text{Pd}/2\text{Au}$, $2\text{Pd}/1\text{Au}$, $1\text{Pt}/2\text{Au}$ and $2\text{Pt}/1\text{Au}$; to investigate the fundamental aspects related with the existence of a bimetallic junction and its influence on the kinetics of the bond breaking of O–O and O–OH to avoid the secondary product (H_2O_2). Although it is out of the scope of the current contribution, H_2O_2 production could also be studied to provide a full insight on the reaction pathways. Corresponding work is in progress in our group.

According to the previous explanation, our results are summarized in Table 2. The corresponding final and transition state configurations as well as the activation energies (in eV) are reported for the bond breaking processes of both precursors on the mixed systems.

Our results show that the dissociation of the adsorbed precursor – $\text{O}_{2(\text{ad})}$ – is a barrierless process on Pd(100) (in accord with other authors [76]), with the two oxygen atoms as the final state located on hollow sites. As expected for the bimetallic material with a larger amount of Pd ($2\text{Pd}/1\text{Au}$), the behavior is similar to that of the pure palladium surface. The initial state is an adsorbed O_2 molecule on an "E" site. Its dissociation takes place with no barrier on the Pd "region", which confirms the higher affinity of O_2 for Pd over Au. At the final state, the oxygen atoms are also situated at the Pd "region"

¹taken as reference materials

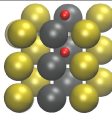
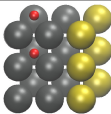
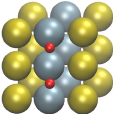
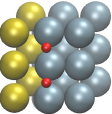
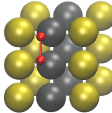
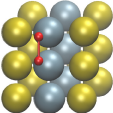
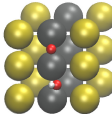
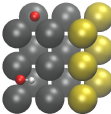
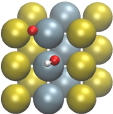
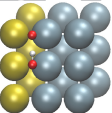
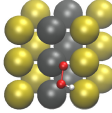
Structures		1Pd/2Au	2Pd/1Au	1Pt/2Au	2Pt/1Au	
Prec						
	O ₂	FS				
		TS				
E_{act}/eV		0.3	0.0	0.1	0.0	
OOH						
	FS					
	TS					
E_{act}/eV		0.1	0.0	0.0	0.0	

Table 2: Final (FS) and transition (TS) state configurations and the corresponding activation energies (E_{act}) for each investigated reaction path. Upper part: the bond breaking process of O₂. An elongated adsorbed oxygen molecule is found at the bimetallic junction. Bottom part: the bond breaking process of OOH. An elongated adsorbed peroxy is found at the bimetallic junction.

on "E" hollow sites (Table 2). For simplicity and in all the studied cases, the corresponding initial state has been taken as reference to recast the energy values, i.e. $E_{ini} = 0$.

The scenario changes notoriously when the amount of Au increases on the bimetallic material in comparison with pure Au. The same phenomenon is now hindered by a barrier of about 0.3 eV on 1Pd/2Au surfaces, whereas on a pure Au surface the process exhibits a barrier higher than 1 eV [64]. On 1Pd/2Au systems, the oxygen molecule is initially adsorbed on a "H" site on the surface, and starts diffusing to the bimetallic interface, where an elongated oxygen molecule has been identified as the transition state (Table 2). At the final state, the two oxygen atoms are located on displaced mixed "C" hollow sites (Table 2), which also shows the preference of O for Pd.

Similar studies have been addressed on nPt/mAu mixed surfaces as well. For 1Pt/2Au surfaces, the adsorbed molecular oxygen ($O_{2(ads)}$) dissociates in two oxygen atoms ($O_{(ads)}$) with a considerably low activation barrier of about 0.1 eV. Similarly to 1Pd/2Au, the molecule initially sits on a "H" site and subtly propagates to the bimetallic interface, where the oxygen bond breaks (Table 2). An elongated O₂ has been also found as a transition state. The final state is shown in Table 2, with the O atoms located on "H" sites.

For 2Pt/1Au, the scission of O–O bond exhibits no activation energy. A situation quite similar in comparison to 1Pt/2Au ($E_{act} \approx 0.1$ eV) and Pt(100), which displays a rather small dissociation barrier ($E_a \approx 0.15$ eV, in agreement with other authors [63]). As in the previous cases, the molecule adsorbs on a "H" site and bond breaking takes place at the bimetallic junction. Finally, the oxygen atoms are favorably adsorbed on "H" sites (Table 2).

Besides the previous scenario, we have also considered the bond breaking step of the adsorbed OOH for the same materials (pure surfaces and the bimetallic materials: nPd/mAu, nPt/mAu) to obtain O_{ad} and OH_{ad} as products. As follows from our results, the higher barrier (≈ 0.3 eV) occurs on a Au(100) surface. For Pd(100) and 1Pd/2Au, the process takes place with nearly no barrier (≈ 0.1 eV). For this bimetallic surface (1Pd/2Au), at the initial state, the OOH is adsorbed on a distorted "H" site. Similarly to the molecular oxygen, the OOH species is re-oriented to the bimetallic interface, where the transition state is identified (Table 2). The final states for both species – O and OH – sit on "H" sites and are shown in Table 2. For higher amount of Pd (2Pd/1Au), the scission occurs in the Pd "region" in the same way as it was described for the molecular oxygen precursor. No activation energy has been found, and as final configurations, the O atom is situated on an "E" site while the OH is located on an "H" one (Table 2).

For the rest of the systems (1Pt/2Au, 2Pt/1Au), the scission is barrierless as in the pure Pt(100) surface [18]. The O–OH breaking takes place at the junction. The corresponding final states are shown in Table 2. The adsorption follows the expected behavior, the O and OH locate preferentially on a "H" site and on an off-center top Pt site for the case of 1Pt/2Au surfaces (Table 2), while for 2Pt/1Au structures, both O and OH sit on mixed Pt–Au bridge sites (Table 2).

4 Discussion

In accord to the reported data [64], the dissociation on Au(100) is unfavorable with an energy barrier higher than 1 eV, which indicates that the ORR would not evolve through the dissociative route. Hence, according to our results, the modification of Au with Pd or Pt rows would lower the barrier for the bond breaking process and favors the dissociative mechanism.

Additionally, it should be emphasized that the breaking of the O–OH bond is a barrierless process for 1Pt/2Au, 2Pt/1Au, 2Pd/1Au surfaces, and an almost barrierless process for 1Pd/2Au configurations; and it would be expected that the hydrogen peroxide reaction does not take place on the investigated materials either. This synergetic behavior for the ORR has already been seen experimentally for PtAu in the work of Brown *et al.*, in which Au–Pt nanoparticles with Pt₅₉Au₄₁ proportions showed charge densities nearly 5 times higher than Pt thin films [77]. A similar behavior was found for this bimetallic combination in the work of Qu *et al.* [78], where a Pt nanofilm decorated gold microelectrode with various Pt/Au surface ratio were studied. The authors concluded that the optimized surface contents of Pt and Au, which demonstrated high activity and high efficiency of Pt usage, was determined as Pt/Au surface ratio of 0.62.

Although many works have shown that the combination of Pd and Au can selectively reduce O₂ to H₂O₂, which makes them suitable electrocatalysts for H₂O₂ synthesis [79, 80], our results suggest that these type of electrodes would potentially reduce O₂ through the 4e⁻ route. In spite of this apparent disagreement, it is known that several factors such as crystallographic orientations, support material, among other characteristics (like size, pH, etc.) can strongly influence the kinetics and mechanism of the ORR, leading to a variation from the 2 to 4 electron process. For instance, in the computational work of Ham *et al.* [81], where PdAu(100) surfaces were also studied, it was found that Pd monomer pairs can greatly enhance the kinetics for the ORR compared with pure Pd(100), which is in agreement with what we have seen for this kind of electrocatalysts.

As it was explained previously, the scission energy can be used to obtain information about the material performance [73]. In this context, our results reveal that the main difference lies in the bond breaking process of the adsorbed precursor –OOH_(ad) and O_{2(ad)}– which avoids hydrogen peroxide formation. In all the studied cases, the activation energy decreases or even disappears compared to pure gold. For those specific processes, where a transition state was found, the corresponding species –OOH and O₂– re-localizes on a mixed site in a parallel direction to the bimetallic interfacial region (Table 2) where the bond scission occurs. Then, a surface diffusion process takes place leading to the final state. It is important to notice that, except for 2Pd/1Au, the bond breaking process of both precursors occurs at the bimetallic junction (i.e. not on top of Pt or Pd (regions), the most active metals for this process). A detailed observation of each reaction path obtained by the NEB method indicates that, for the scission to take place, the precursors must be localized in a parallel way respect to the heteroatomic line. Therefore, a material with a bimetallic geometrical arrangement that presents an interfacial line with different sites, such as the one proposed in this contribution, or for instance, embedded mosaics of Pt or Pd in a Au substrate, which allow the precursor to localize parallel over the junction, can be considered as possible electrocatalysts for the reaction.

From our knowledge, our intercalated bimetallic model originates a new reaction environment – heteroatomic interfacial line – that has not yet been investigated by computational means. Instead a rather similar reported structure such as a monolayer of Pt on a Au(111) surface can be cited. Nilekar *et al.* [44] reported an activation barrier of 0.51 eV for the molecular oxygen dissociation on a Pt ML on Au(111), which is lower than that for the bare Pt(111) surface (≈ 0.77 eV). Another interesting approach was made by Zhang *et al.* [69], where a monolayer of Pt and another transition metal was deposited on top of a Pd(111) single crystal. According to the authors these electrocatalysts have a high activity compared to pure Pt for ORR. It is interesting to highlight that the improvement on the activity of the catalyst was attributed by the authors to the lowering of OH coverage due to the presence of the neighbor surface metal atom (in this case, Ir, Ru, Re, or Os). This kind of contribution, i. e. the modification of the metal catalytic behavior due to the presence of a foreign metal on the surface, is the kind of synergetic effect seen on the catalysts studied in this work. Nonetheless, according to Zhang *et*

al. [69], the combination of Au and Pt in the mixed monolayer decrease the ORR kinetics in comparison with a pure Pt monolayer, which is in contrast to what we have found for the Au-Pt system studied in this article. In spite of this, several experimental works found a synergetic effect for mixed Au-Pt systems [82, 83] and the difference in these results could arise from the dissimilarities in the superlattice structure studied herein.

Moreover, electronic and geometrical factors that affect the material reactivity exist in both models, the prime difference in our proposed configuration is the existence of an exposed bimetallic interface for the reaction to occur, which may favor some processes over others, for example, to avoid the formation of secondary products.

5 Conclusions

The oxygen reduction reaction on bimetallic electrodes based on the combination of Au with M (M: Pd or Pt), considering 1:2 and 2:1 ratios, was studied. Interestingly, it was found that even for the highest Au ratios studied, the reactivity behavior of these materials shared more similarities with Pt or Pd bare metals than with bare Au. This trend was established by electronic, geometrical and kinetic studies, considering the adsorption and the O–O bond breaking for O_2^* and OOH^* intermediates. For some combinations, adsorption energies towards these intermediates are greater (more negative values) than for bare Pt or Pd metals, providing evidence of a synergetic behavior between Au and M. Our results suggests not only that Pt loadings could be reduced without losing much catalytic activity towards the orr if properly combined with gold, which is not a great benefit considering Au is also a highly expensive metal, but could actually enhance the oxygen reduction reaction rate, although this last statement needs further research. On the other hand, our results imply that Pd-Au, mixed in a proper ratio, can also be a great electrode material for orr, nevertheless its catalytic properties seems to be behind the Pt-based electrodes. Further investigations are being conducted in order to elucidate the mechanism of the orr in intercalated Rh/Au electrodes.

Acknowledgements

Financial support by CONICET and Universidad Nacional del Litoral is gratefully acknowledged. P.Q. thanks PICT-2014-1084 for support. The authors also thank the support given by Santa Fe Science Technology and Innovation Agency (ASACTEI, grant 00010-18-2014). The authors thank to Prof. V. Marzocchi for his contribution with computing resources.

References

- [1] Santos E. and Schmickler W. Interfacial Electrochemistry. Springer-Verlag, 2nd edition, 2010.
- [2] Santos E. and Schmickler W. Electrocatalysis; from fundamental aspects to fuel cells. Wiley, New York, 2011.
- [3] Vielstich W., Hamann C.H., and Hamnett A. Electrochemistry. Wiley-VCH, New York, 2007.
- [4] Koper M.T.M. Fuel Cell Catalysis. Wiley-VCH, New York, 2009.
- [5] Lipkowski J. and Ross P.N. Electrocatalysis. Wiley-VCH, New York, 1998.
- [6] Marković N.M., Adžić R.R., Cahan B.D., and E.B. Yeager. Journal of Electroanalytical Chemistry, 377:249, 1994.
- [7] Shao M., Peles A., and Shoemaker K. Nano Lett., 11:3714, 2011.
- [8] Mayrhofer K.J.J., Blizanac B.B., Arenz M., Stamenkovic V.R., Ross P.N., and Marković N.M. J. Phys. Chem. B, 109:14433, 2005.
- [9] Shim J.H., Kim J.E., Cho Y.B., Lee C., and Lee Y. Phys. Chem. Chem. Phys., 7:15365, 2013.
- [10] Dai L., Xue Y., Qu L., Choi H-J., and Baek J-B. Chem. Rev., 115:4823, 2015.
- [11] Jiang W-J., Gu L., Li L., Zhang Y., Zhang X. Zhang L-J., Wang J-Q., Hu J-S., Wei Z., and Wan L-J. J. Am. Chem. Soc., 138:3570, 2016.

- [12] Byon H.R., Suntivich J., and Shao-Horn Y. Chem. Mater., 23:3421, 2011.
- [13] Venarusso L.B., Bettini J., and Maia G. Journal of Solid State Electrochemistry, 20:1753, 2016.
- [14] Kobayashi S., Wakisaka M., Tryk D.A., Iiyama A., and Uchida H. J. Phys. Chem. C, 121:11234, 2017.
- [15] Hartl K., Mayrhofer K.J.J., Lopez M., Goia D., and Arenz M. Electrochem. Commun, 12:1487, 2010.
- [16] Guo S., Zhang S., and Sun S. Angew. Chem. Int. Ed., 52:2, 2013.
- [17] Watanabe M., Tryk D. A., Wakisaka M., Yano H., and Uchida H. Electrochim. Acta, 84:187, 2012.
- [18] Ford D.C., Nilekar A.U., Xu Y., and Mavrikakis M. Surf. Sci., 604:1565, 2010.
- [19] Gasteiger H.A., Kocha S.S., Sompalli B., and Wagner F.T. Applied Catalysis B: Environmental, 56:9, 2005.
- [20] Stacy J., Regmi Y.N., and Leonard F.M. Renewable and Sustainable Energy Reviews, 69:401, 2017.
- [21] Holton O.T. and Stevenson J.W. Platinum Metals Rev., 57:259, 2013.
- [22] Antolinia E., Zignani S.C., Santos S.F., and Gonzalez E.R. Electrochim. Acta, 56:2299, 2011.
- [23] Zhao J., Jarvis K., Ferreira P., and Manthiram A. Journal of Power Sources, 196:4515, 2011.
- [24] Stamenkovic V.R., Fowler B., Mun B.S., Wang G., Ross P.N., and Lucas C.A. Markovic N.M. Science, 315:493, 2007.
- [25] Su L., Jia W., Li C.M., and Lei Y. ChemSusChem, 7:361, 2014.
- [26] Santos E. and Schmickler W. Catalysis in Electrochemistry. From fundamentals to Strategies for Fuel Cell Development. Wiley-VCH, Weinheim, 2005.
- [27] Hammer B. and J. Norskov J. Ad. in Catalysis, 45:71, 2000.
- [28] Quaino P.M., Gennero de Chialvo M.R., and Chialvo A.C. J. Electrochem. Soc., 156:B167, 2009.
- [29] Mo Y. Shang J., Vukmirovic M.B., Klie R., Adzic R.R., and Sasaki K. J. Phys. Chem. B, 108:10955, 2004.
- [30] Zubimendi J.L., Andreassen G., and Triaca W.E. Electrochim. Acta, 40:1035, 1995.
- [31] Zinola F., Castro Luna A.M., Triaca W.E., and Arvia A.J. Electrochim. Acta, 39:1627, 1994.
- [32] Zhang J., Lima F.H.B., Shao M.H., Sasaki K., Wang J.X., Hanson J., and Adzic R.R. J. Phys. Chem. B, 108:22701, 2005.
- [33] Montero M.A., Gennero de Chialvo M.R., and Chialvo A.C. J. Hydrogen Energy, 36:3811, 2011.
- [34] Zhu T. and Ertekin E. Phys. Rev. B, 90:195209, 2014.
- [35] Ma W., Ma R., Wang C., Liang J., Liu X., Zhou K, and Sasaki T. ACS Nano, 9:1977, 2015.
- [36] Kang Y., Ye X., Chen J., Cai Y., Diaz R.E., Adzic R.R., Stach E.A., and Murray C.B. J. Am. Chem. Soc., 135:42, 2013.
- [37] Rau M.S., Gennero de Chialvo M.R., and Chialvo A.C. Journal of Power Sources, 216:464, 2012.
- [38] Luque G., Gennero de Chialvo M.R., and Chialvo A.C. J. Solid State Electrochem., (10.1007/s10008-015-2987-4), 2016.
- [39] Zhang J., Sasaki K., Sutter E., and Adzic R.R. Science, 315:220, 2007.
- [40] Dumesic J.A., Plauck A, Stangland E. E., and Mavrikakis M. Proceedings of the National Academy of Sciences, 113:E1973, 2016.
- [41] Petkov V., Wanjala B.N., Loukrakpam R., Luo J., Yang L., Zhong C-J., and Shastri S. Nano Lett., 12:4289, 2012.
- [42] Ponc V and Bond G.C. Catalysis by metals and alloys. Elsevier, Amsterdam, 1995.
- [43] Bond G.C. Platinum Metals rev., 51:63, 2007.
- [44] Nilekar A.U., Zhang Y.Xu, Vukmirovic M.B., Sasaki K., Adzic R.R., and Mavrikakis M. Top Catal., 46:276, 2007.

- [45] Escaño MC, Gyenge E, Nakanishi H, and Kasai H. J. Nanosci. Nanotechnol., 4:2944, 2011.
- [46] Shao MH, Huang T, Liu P, Zhang J, Sasaki K, Vukmirovic MB, and Adzic RR. J. Nanosci. Nanotechnol., 5:10409, 2006.
- [47] Kresse G. and Hafner J. Phys. Rev. B, 47:558–561, 1993.
- [48] Kresse G. and Furthmuller J. Comput. Mater. Sci., 6:15–50, 1996.
- [49] Kresse G. and Furthmuller J. Phys. Rev. B, 49:14251–14269, 1994.
- [50] Blochl P. E. Phys. Rev. B, 50:1795317979, 1994.
- [51] Kresse G. and Hafner J. J. Phys. Condens. Matter., 6:8245–, 1994.
- [52] Vanderbilt D. Phys. Rev. B, 41:78927895, 1990.
- [53] Kresse G. and Joubert D. Phys. Rev. B, 59:1758–1775, 1999.
- [54] Wang Y. and Perdew J.P. Phys. Rev. B, 44:13298, 1991.
- [55] C. Kittel. Introduccion a la fisica del estado solido. Editorial Reverte, S.A., espanol edition, 1975–1976.
- [56] Luo J., Maye M.M., Petkov V., Kariuk N.N., Wang L., Njoki P., Mott D. Lin Y., and Zhong C.J. Chem. Mater., 17:3086, 2005.
- [57] Monkhorst H.J. and Pack J.D. Phys. Rev. B, 13:5188, 1976.
- [58] Henkelman G., Uberuag B.P., and Jonsson H. J. Chem. Phys., 113:9901, 2000.
- [59] Henkelman G. and Jonsson H. J. Chem. Phys., 113:9978, 2000.
- [60] Van Brussel M., Kokkinidis G., Vandendael I., and Buess-Herman C. Electrochemistry Communications, 4:808, 2002.
- [61] Koenigsmann C., Sutter E., Chiesa T.A., Adzic R.R., and Wong S.S. Nano Lett., 12:20, 2013.
- [62] Alia S.M., Duong K., Liu T., Jensen K., and Yan Y. ChemSusChem, 7:1739, 2014.
- [63] Duan Z. and Wang G. Journal of Physical Chemistry C, 117:6284, 2013.
- [64] Nazmutdinov R. Santos E., Quaino P., Luque N., and Schmickler W. Angewandte Chemie Int. Ed., 51:12997, 2012.
- [65] Niemantsverdriet J. W., Hussain A., Gracia J., and Nieuwenhuys B. E. The Journal of Physical Chemistry B, 107:9298, 2013.
- [66] Santos E., Quaino P., and Schmickler W. Electrochim. Acta, 55:4346, 2010.
- [67] Stephens I.E.L., Bondarenko A.S., Grønbjerg U., Rossmeisl J., and Chorkendorff I. Energy Environ. Sci., 5:6744, 2012.
- [68] Gross A. Topics in Catalysis, 37:29, 2006.
- [69] Zhang J., Vukmirovica M.B., Sasaki K., Nilekar A.U., Mavrikakis M., and Adzic R.R. J. Am. Chem. Soc., 127:12480, 2005.
- [70] Sha Y, Yu T.H., Merinov B. V., and Goddard III W. A. ACS Catal., 4:1189, 2014.
- [71] Strasser P., Koh S., and Greeley J. Physical Chemistry Chemical Physics, 10:3670, 2008.
- [72] Jalili S., Zeini A., and Habibpour I.R. International Journal of Industrial Chemistry, 4:33, 2013.
- [73] Bligaard T., Nørskov J.K., Dahl J., Matthiesen J., Christensen C.H., and Sehested J. Journal of Catalysis, 224:206, 2004.
- [74] Arce M. and Fernández J. Electrochim. Acta, 10:953, 2015.
- [75] Fantauzzi D., Zhu T., Mueller J.E., Filot I.A.W., Hensen E.J.M., and Jacob T. Catal. Lett., 145:451, 2015.
- [76] Liu D.J. and Evans J.W. Physical Review B, 89:205406, 2014.

- [77] Brown B., Wolter S.D., Stoner B.R., and Glass J.T. Journal of The Electrochemical Society, 155:B852, 2008.
- [78] Qu D., Tao Y., Guo L., Xie Z., Tu W., and Tang H. Int. J. Electrochem. Sci., 10:3363, 2015.
- [79] Edwards J.K., Freakley S.J., Carley A.F., Kiely C.J., and Hutchings G.J. Acc. Chem. Res., 47:845, 2014.
- [80] Pizzutilo E., Kasian O., Choi C.H., Cherevko S., Hutchings G.J., Mayrhofer K.J.J., and Freakley S.J. Chemical Physics Letters, 683:436, 2017.
- [81] Hama H.C., Hwanga G.S., Hanb J., Yoonb S.P., Namb S.W., and Lim T.H. Catalysis Today, 263:11, 2016.
- [82] Tripkovic V., Hansen H.A., Rossmeis J., and Vegge T. Phys. Chem. Chem. Phys., 17:11647, 2015.
- [83] He L-L., Zheng J-N., Song P., Zhong S-X., Wang A-J., Chen Z., and Feng J-J. Journal of Power Sources, 276:357, 2015.

Highlights

- orr is investigated on different ratios of Pd-Au and Pt-Au bimetallic electrodes
- A heteroatomic junction is defined as a new reaction environment
- The kinetics of the O-O (O-OH) bond breaking is studied at the heteroatomic junction
- For Au-M with lower M ratios, the barriers for O-O scission suggest a reactive surface towards the orr
- The O-OH scission is nearly barrierless, implying that the O₂ reduction proceeds via the full reduction to H₂O

ACCEPTED MANUSCRIPT

MANUSCRIPT

